Adaptive window algorithm for aerial image stereo

Jean-Luc Lotti, Gerard Giraudon

INRIA

INSTITUT NATIONAL DE RECHERCHE EN INFORMATIQUE ET EN AUTOMATIQUE

Adaptive Window Algorithm for Aerial Image Stereo

Jean-Luc LOTTI
Gérard GIRAUDON

N° 2121
Novembre 1993

PROGRAMME 4

Robotique, image
et
vision

Rapport de recherche

1993

Adaptive Window Algorithm for Aerial Image Stereo

Jean-Luc LOTTI* & Gérard GIRAUDON**

Programme 4 - Robotique, Image et Vision

Projet PASTIS

Rapport de recherche n°2121- 16 Novembre 1993

24 pages

Abstract: Binocular stereo vision processes estimate 3D surfaces using a pair of images taken from different points of view. For that, 3D surface characteristics are estimated by matching 2D image areas or features corresponding to the projections of same 3D points. The most classic area-based methods used cross correlation with a fixed window-size, but this technique presents a major drawback: the computation of depth is generally prone to errors close to surface discontinuities.In this paper, we present our current work on aerial stereo images of urban areas. A correlation-based algorithm with an adaptive window-size constrained by an edge map extracted from the images is presented. The algorithm follows 4 steps: first window sizes for each pixel are computed; then a disparity map is created; third, map completion is performed and finally a final dense disparity map with subpixel precision is produced. Experimental results on real aerial images are presented

Key-words: High resolution, aerial image, stereo vision, correlation, adaptive window, disparity limits.

(Résumé : tsvp)

* Jean-Luc.Lotti@sophia.inria.fr
** Gerard.Giraudon@sophia.inria.fr

Unité de recherche INRIA Sophia Antipolis
2004 route des Lucioles, BP 93, 06902 SOPHIA-ANTIPOLIS Cedex (France)
Téléphone : (33) 93 65 77 77- Télécopie : (33) 93 65 77 65

Algorithme à Fenêtre Adaptative pour Image Stéréo Aérienne

Résumé : Les processus de stéréo vision binoculaire estiment les surfaces 3D en utilisant une paire d'images prises à partir de points de vue différents. Pour cela, les caractéristiques de la surface 3D sont estimées par la mise en correspondance de zones ou de primitives de l'image 2D, correspondantes aux projections des mêmes points 3D. Les méthodes les plus classiques, utilisent la corrélation croisée avec une fenêtre de taille fixe, mais cette technique présente un problème majeur: Le calcul de la profondeur est généralement erroné près des discontinuités de surface. Dans ce rapport, nous présentons notre travail actuel sur des images stéréo aériennes en zones urbaines. Un algorithme de corrélation avec fenêtre adaptative contrainte par une carte de contours extraite des images est présenté. L'algorithme suit 4 étapes: premièrement les tailles des fenêtres sont calculées pour chaque pixel; puis une carte de disparité est crée; troisièmement, on complète la carte et finalement une carte de disparité dense avec une précision sub-pixellique est produite. Les résultats sur des images aériennes réelles sont présentés.

Mots-clé : Haute résolution, image aérienne, stéréo vision, corrélation, fenêtre adaptative, limites de disparité.

Table des matières

1 Introduction

This paper addresses the Stereo Vision problem in the domain of 3D aerial image reconstruction *. In this domain, image resolution is generally less than one meter. So, the assumption of the world surface continuity is wrong, and we have to take into account 3D surface discontinuities such as buildings, trees... This domain is usually relevant to High Resolution Stereovision domain.
More precisely, we want to obtain a 3D surface reconstruction presenting discontinuities, well localized, for a building and in the same time, presents a good regularity for the smooth surfaces of the ground. In fact, we have to solve a mix stereovision problem, intermediate between typically indoor and satellite images.
3D informations leading to cartographic environments, may be computed either by active techniques (ultra-sound, laser or radar range finger) or by passive techniques (triangulation by stereovision). Active technique such a laser range finder, gives a good accuracy but a sparse map of 3D environment. Generally, passive techniques are used to obtain dense map. Among passive approaches, there are shape-from-shading and more generally shape-from-X, structure-from-motion and of course stereovision with bi or trinocular images. In the case of stereovision process, a good accuracy on results requires a large B/H ratio, while matching (to reduce false matches) requires a small B/H ratio.

Most existing techniques are distinguished by the choice of features, and associated constraints. One generally sorts matching algorithms in two large families:

- Area-based methods [2][4][8][14] (Region-Based Stereo) Pixel radiometry used by correlation algorithm giving dense map, superior in information from texture but with bad localisation of depth discontinuity and badly checking invariability propriety by changing point of view.

- Feature-based methods [1][2][3][9] (Pixel and Contour-Based Stereo) Salient Points, Contours Chains, Lines Segments or Polynomials Curves giving no dense map but a good localisation of depth discontonuity.

All these features are related with constraints which are for the most part:

> Epipolar Geometry, Maximum and Minimum Disparity Gap, Local Attribute, Singleness, Disparity Continuity (in most algorithms there is no rough disparity variation),...

In terms of matching techniques, different methods are been proposed to solve stereovision problem under these constraints:

- ✯ Cross Correlation
- ✯ Dynamical Programming
- ✯ Graph Isomorphism
- ✯ Relaxation

* This research is supported by PACA and ESTEC contracts.

- ★ Prediction-Verification
- ★ Voting Technique
- ★ Hierarchical Techniques
- ★ Simulated Annealing

Notice that no stereo vision algorithm solves the problem completely and each method presents different advantages and drawbacks. The main problems which occur in stereovision matching are due to occultations, noise in the images, or reflections and any change between the images.

To compute a Dense Depth Map, the classical method is to start with a correlation-based matcher followed by a surface interpolation or approximation of disparity map, to obtain a full surface [4][14]. In this case, most programs use a fixed window-size. In the case of 3D continuity surface and textured images, this method gives good results. But, we observe that for small windows, it does not cover enough intensity variation, and for large ones, problems appear near disparity discontinuities and occluded regions.

To alleviate these problems, T. Kanade and M. Okutomi propose in [10][11] and [12] to correcte an initial disparity by adapting the window size to the local variations of the image intensity and disparity. Their method controls not only the size but also the rectangular shape of the window.

We have implemented this technique and after testing, we noted that the surface boundaries did not correspond well to physical ones.

The reason is that the computed window is based on an initial disparity map obtained by classical cross correlation which is false at discontinuity localization. This solution gives good disparity correction only if we have good initial discontinuity location, but does not solve the problem if we have not.

So to prevent this problem, we need a good localization of the discontinuities in initial disparity map.

In their article [3], R.Chung and R.Nevatia exploit structural features to recover discontinuity information and show the importance of image contours. Many other articles show the same facts [2]and [6].

We propose here, a contour constrained window correlation algorithm to obtain the initial disparity map with good discontinuities localization, followed by the Kanade correction algorithm.

We present below in detail:

Firstly, adaptive window size computation constrained by contours and a maximal possible size fixed here at (7x7).

Secondly, for each image point, the disparity computation with pixel precision from the «disparity limits» of the four non centered adaptive window associated to him.

Thirdly, the disparity map completion using iteratively: filtering, left-right validating and filling stages.

Finally, dense disparity map with subpixel precision by Kanade correction algorithm on initial completed map and good discontinuity localization.

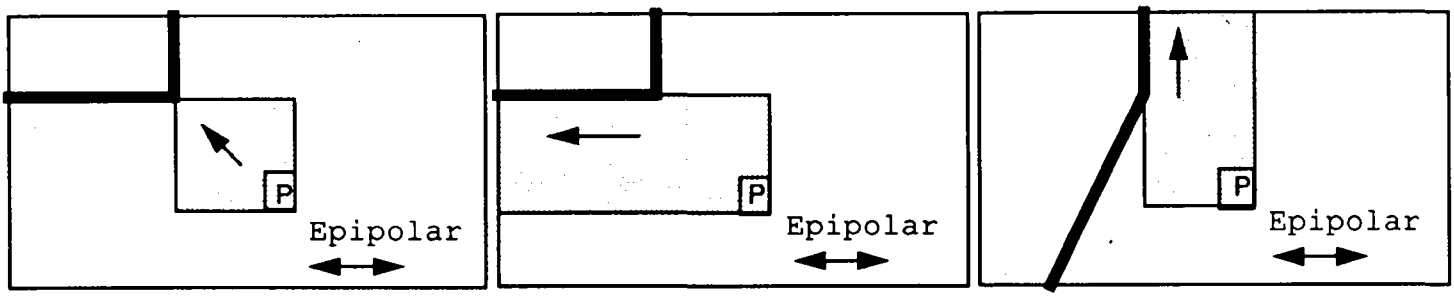

Figure 1 : Window growing steps (Black line is contour, P the observed pixel in the right down corner): a) maximum square from P. b) grow parallel to epipolar line if possible. c) try perpendicular side if (b) is not possible.

In the following sections, we assume that the right image as been corrected to yield corresponding epipolar lines between the two images.

2 Window Size Computation

To deal with contours, we first extract edges from the image using a Canny-Deriche filter and eliminate noise by thresholding the edges with hysteresis filter shown in (Image 1). Many ideas may by used to detect contours and adjust hysteresis thresholds like in [15], here we rely on heuristics.
We notice that disparities are different on each side of a depth (Z) discontinuity contour, but this is not true for a texture contour. Here we introduce the fact that discontinuities and occlusion generate contours which must constrain the size of the adaptive window in the correlation algorithm (Image 2). If we observe the contours in the left and right images, we can see that they are different. This shows that the relative motion of contours indicates occlusion, producing another important piece of information: We need to use the smallest limited contour window between left and right images (Image 3) to compute the disparity. Doing this we avoid to use occluded pixels in the correlation score computation.
We will see later how to compute disparity from what we define as «Disparity Limits», using for each pixel P in the image four excentred windows (Image 4).

Consequently to find the size of a Constraint Window associated to the pixel P (X,Y coordinates) in the left image, we use three stages Figure 1 :

- the window grows diagonally first in order to find the largest possible square: maximum square between pixel P and contours, in a direction depending on which of the four corners is being considered.
- we then try to grow the square window in the epipolar direction: rectangular shape with largest side parallel to the epipolar line.

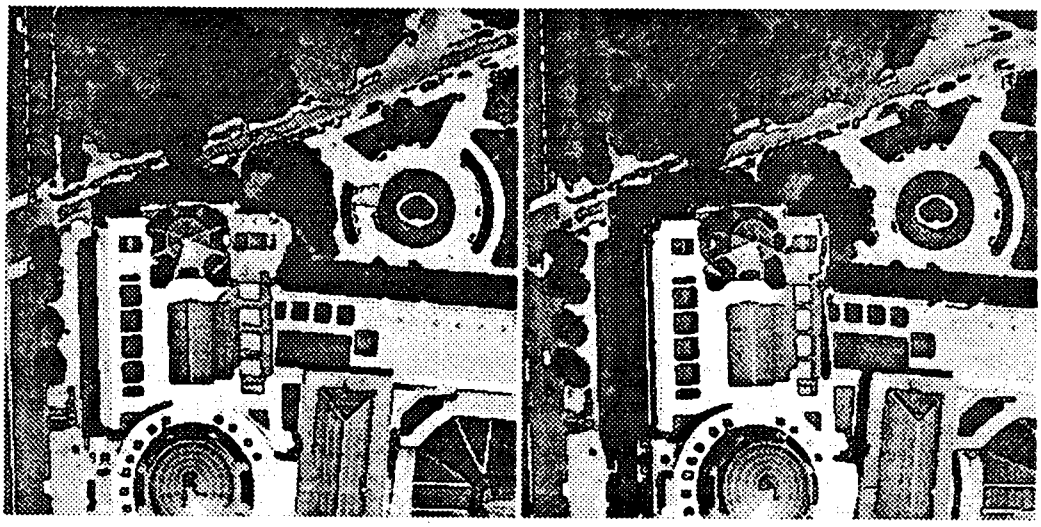

Image 1 left and right Contours with intensity, image 400x400 of Grand-Palais (Paris).

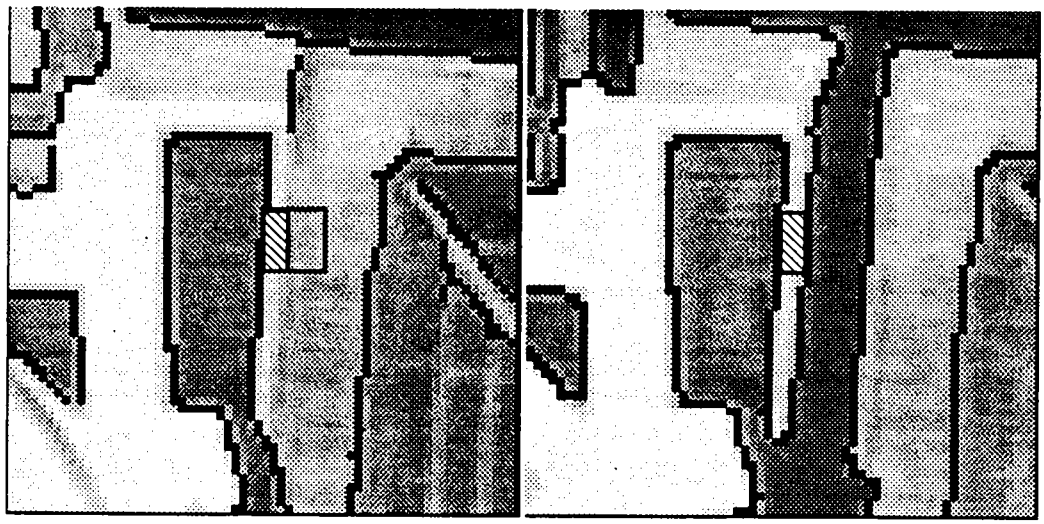

Image 2 The contours of the right image constrain the window size in the left one.

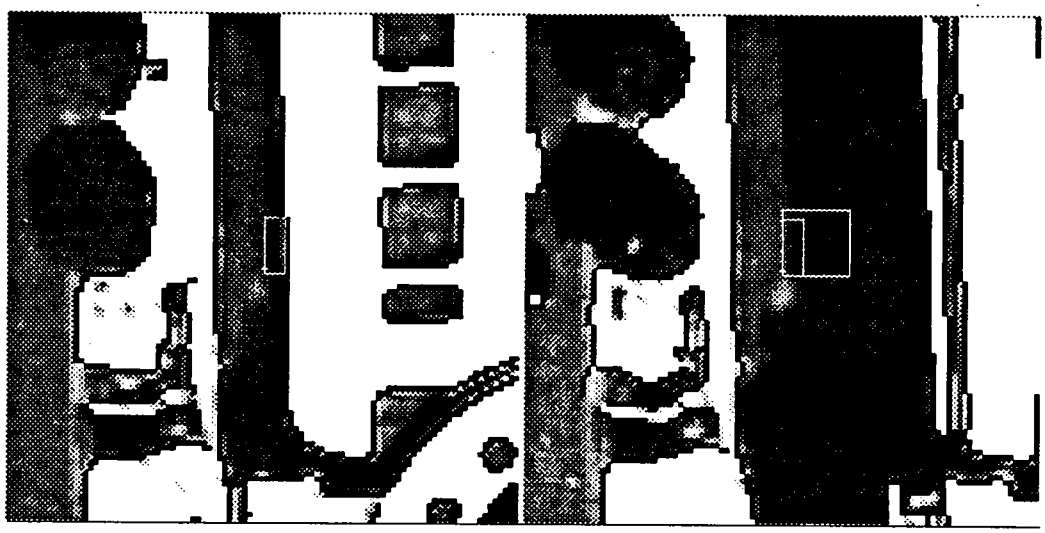

Image 3 Relative motion of contours indicates an occluded area. So we need to take the smallest limited window.

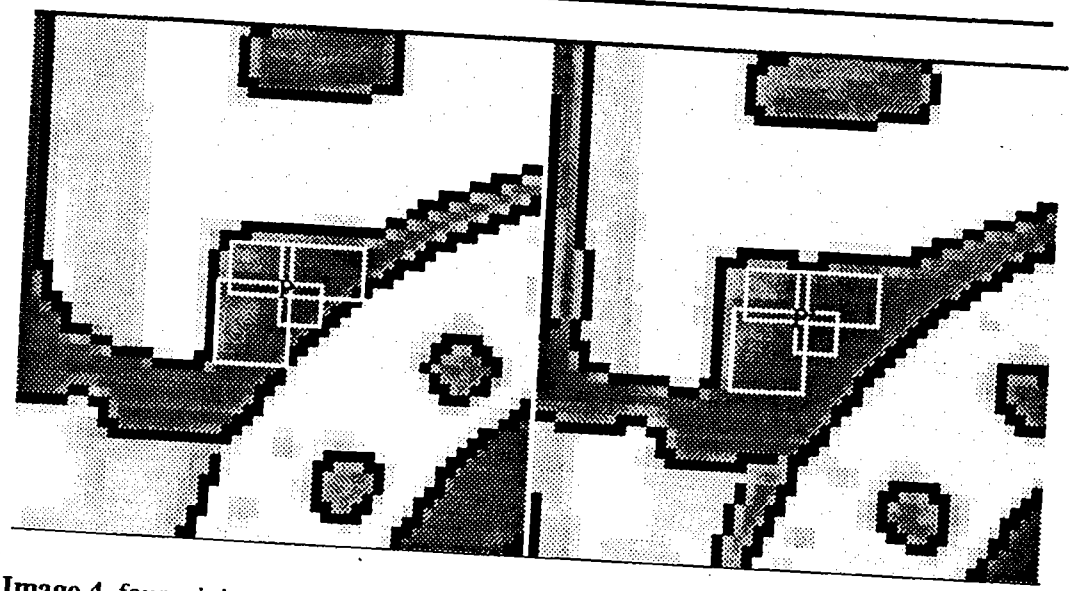

Image 4 four minimal windows associated to the pixel P for disparity d.

- if we can't grow in the epipolar direction (because of a contour), we try the perpendicular one:
  rectangular shape with largest side perpendicular to the epipolar line.

We have then a maximal window for P in the left image.

Now from the minimal and maximal depth estimations we know that disparity **d** is in a range [dmin,dmax].
To obtain the right maximal window for the couple (P,d), for each disparity value **d**, the same window size computation is done for the pixel P' (associated to P as X'=X+d) in the right image.
We have then for each possible disparity value **d** a right maximal window for P. For each disparity value **d**, we may to compute the minimal window for P (Image 2) and (Image 3) by the overlap between the left and right maximal windows.
Then for each couple (P,d) we have a minimal window.

3 Disparity Computation

We notice that between two Z discontinuity contours, the disparity is locally constant (there is no large discontinuity). We compute four minimal windows for each couple (P,d), where pixel P is in a different corner of each window (Image 4). We choice four windows because computation is easily done and most of discontinuities may be detected. We compute the correlation score associated to each window. This defines four «disparity limits» which give a Final correlation score F(P,d), and hence D(P) the disparity map.

3.1 Disparity Limit

For one point P and for each disparity value d, we have now to compute four «Limits of disparity» scores.

Computation of the score is based on modified classical criteria $C(X, Y, d)$ (covariance, variance based). C(X,Y,d) is in the range [-1,1], and was used by P.Fua [4] for grey level images:

$$C(I_L, I_R) = \frac{covariance(I_L, I_R)}{\sqrt{variance(I_L) \times variance(I_R)}} \tag{1}$$

$$PhiL = (I_L(X+i, Y+j) - \overline{I_L(X, Y)}) \tag{2}$$

$$PhiR = (I_R(X+d+i, Y+j) - \overline{I_R(X+d, Y)}) \tag{3}$$

$$covariance(I_L, I_R) = \frac{\sum_i \sum_j (PhiL \times PhiR)}{Nb_{pt}} \tag{4}$$

$$variance(I_L) = \frac{\sum_i \sum_j PhiL^2}{Nb_{pt}} \qquad variance(I_R) = \frac{\sum_i \sum_j PhiR^2}{Nb_{pt}} \tag{5}$$

$$C(X, Y, d) = \frac{\sum_i \sum_j (PhiL \times PhiR)}{\sqrt{\sum_i \sum_j PhiL^2} \sqrt{\sum_i \sum_j PhiR^2}} \tag{6}$$

where $\overline{I_L(X, Y)}$ and $\overline{I_R(X+d, Y)}$ are the left and right average values of intensity over the window.
Window of Nb_{pt}=((W$_x$ +1)*(W$_y$+1)) pixels, where W$_x$ (W$_y$) are respectively the x axis (y axis) size of it.

Using this classical correlation scheme we obtain a matching disparity value which has the maximum score, but this is for one fixed window-size, and here we have four windows with different sizes.
So we decide first to normalize the score in the range [0,1], which is easily done.

Next, we introduce a distance between the observed pixel P (X,Y) and pixels p_{ij} present in the window.
In order to make the score independent of the window size, we normalize it in the following way:

$$dist(P,p) = \sqrt{distx(P,p)^2 \cdot disty(P,p)^2} \tag{7}$$

$$distx(P,p) = \frac{|X-x|}{W_x} \qquad disty(P,p) = \frac{|Y-y|}{W_y} \tag{8}$$

$$C_w(X,Y,d) = \frac{\sum_i \sum_j \left(\frac{PhiL \times PhiR}{dist(P,p_{ij})}\right)}{\sqrt{\sum_i \sum_j \frac{PhiL^2}{dist(P,p_{ij})}} \sqrt{\sum_i \sum_j \frac{PhiR^2}{dist(P,p_{ij})}}} \tag{9}$$

The window score values obtained are normalized (size independent), also we may obtain a small window with an higher score value than a big one. To favour the biggest window, we then multiply the validated window score values by a window-size coefficient $\frac{Nb_{pt}}{Nb_{max}}$

giving Disparity Limit score:

$$C_w(P,d) = \frac{Nb_{pt}}{Nb_{max}} \cdot (C_w(X,Y,d) - C_{wS}) \tag{10}$$

where C_{wS} is the correlation score threshold.

3.2 Disparity Limit validation: V_w

At this stage we have four «Disparity Limits» scores C_{window} noticed $C_w(P,d)$, but some of them may be bad due to noise or lack of texture in the window. The next three sections describe how to «validate» each of the four window scores, using a boolean value V_{window} noticed V_W and defined by thresholding as:

$$V_W = V_N \cdot V_T \cdot V_C \tag{11}$$

3.2.1 Noise validation: V_N

Assuming that noise for a single image is zero mean Gaussian distributed with variance σ_N^2 we have for the difference between the two images a variance $\sigma_T^2 = 2\sigma_N^2$ with:

$$Probability(-3.09 \cdot \sigma_T < N_w < 3.09 \cdot \sigma_T) = 0.998 \tag{12}$$

So we compute for each minimal window, a difference estimation N_w :

$$N_w = \frac{Nb_{pt}}{Nb_{max}} \cdot \frac{\sum |I_L(P) - I_R(P')|}{Nb_{pt}} \tag{13}$$

where $\frac{\sum |I_L(P) - I_R(P')|}{Nb_{pt}}$ is the mean of the intensity difference (left-right) for each pixel of the minimal window, and $\frac{Nb_{pt}}{Nb_{max}}$ is a coefficient to favour small window because it is more interesting for the same value of noise (Nb_{max} is the number of pixels in a window of maximal size not limited by contours, 7x7 in practice).

giving a boolean value V_N = true if $-3.09 \cdot \sigma_T < N_w < 3.09 \cdot \sigma_T$

3.2.2 Texture validation: V_T

We use a correlation score dealing with signal variation, but some part of the scene may be free of it, so we didn't validate a window without texture or «local variation» as Cochran and Medioni in their article [2].
We classify windows in three categories, textured area, non textured area with strong mean intensity (clear area), and non textured area with low mean intensity (dark area).

This classification is based on texture estimation T_{window} noticed T_w and defined by

$$T_w = \frac{1000}{W_y} \cdot \sum_{r=1}^{W_y} \left(1 - \frac{\bar{x}_r}{\sqrt{(\frac{n-1}{n})\sigma_r^2 + \bar{x}_r^2}} \right) \tag{14}$$

where the variance σ_r^2 and the mean $\bar{x}_r$ are computed along each row r of the window.

The average intensity M_{window} noticed M_w is define by

$$M_w = \frac{\sum \bar{x}_r}{w_y} \tag{15}$$

we classify as:

textured area if $(T_{wS} \le T_w)$

clear area if $(T_w < T_{wS}) \cdot (M_{wS} \le M_w)$

dark area if $(T_w < T_{wS}) \cdot (M_w < M_{wS})$

Then boolean value $V_T = true$ if it is not a dark area.

3.2.3 Correlation Score validation: V_C

boolean value V_C = true if $0 \le C_w(X, Y, d)$.

3.2.4 Threshold estimation

Boolean window validation V_w is based on N_{window}, T_{window}, M_{window}, and C_{window} thresholding:

- Texture threshold is chosen so that $T_{wS} \approx 0.4$ on the left image.
- Intensity threshold M_{wS} is the mean intensity of the left image.
- Noise variance is also found by testing the image $\sigma_N \approx 10$, but it may be also compute on window by noise estimation from each pixel using average, median filter or other different methods as in Olsen article [13].
- Correlation Score is estimated valid upper 50% $C_{wS} = 0.5$.

Image 5 Disparity map 400X400, a) with «Contour Based Disparity Limits» on left image, b) same on right image, c) after left-right validation (from a and b images).

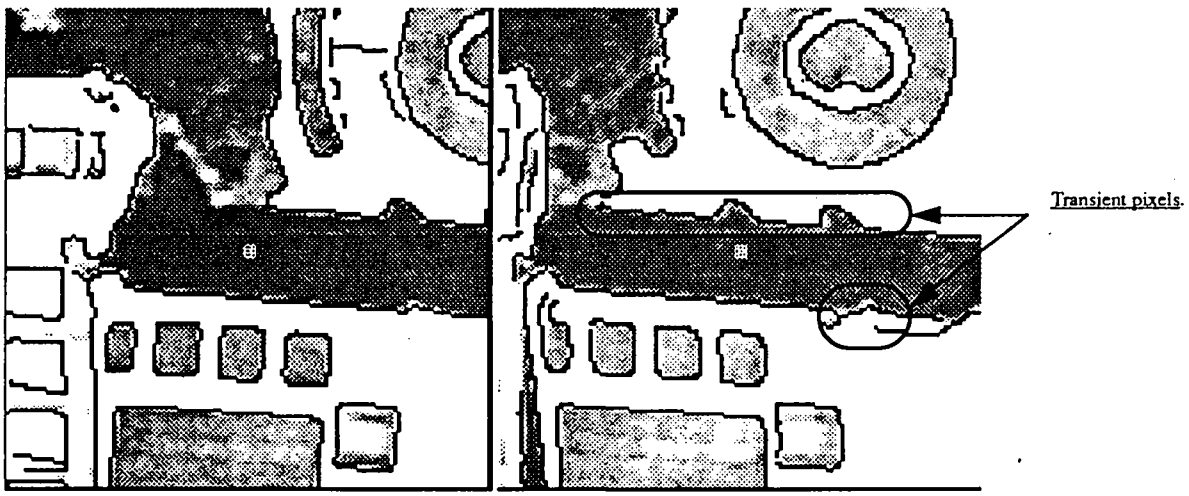

Image 6 «Transient Pixels» white pixels in shadow zone near the Deriche contour on right and left images giving bad matching because they are take in account for window score.

Image 7 Disparity maps with largest contours (left map, right map, validated left-right map), thresholding: Noise=10, Texture=0.5, Correlation=0.7, d=[-1,50].

3.3 Final Score and Disparity Map.

From now, we may compute for each disparity value **d** in [dmin,dmax] the Final score F(P,d) by adding the «Disparity Limits» validated scores:

$$F(P,d) = \frac{NbV}{4} \sum_{w=1}^{4} (V_w \cdot C_w(P,d)) \qquad (16)$$

where *NbV* is the number of validated scores.
The maximum of the function F(P,d) for **d** in [dmin,dmax] gives the disparity value of pixel P, so we obtain a disparity map of left image pixels D(P) (Image 5)a. If we do the same treatement for the right image we obtain a disparity map of right image pixels D'(p') (Image 5)b and may verify that pixel P in the left image has nearly the same disparity value (opposite sign, D(P)=-D'(P')) [4] that matched pixel $P' = P + D(P)$ in right image (Image 5)c.
We see on the disparity map that we have some problems near contours from what we may call «transient pixels» (Image 6) which are not detected by Deriche contour algorithm. To prevent it we use wide contours (three pixels instead of one) and obtain a new disparity map (Image 7). This is not an ideal solution since some transient pixels are not included in the new contours. Local extrema of second derivative may be better to characterize contours limits [5].

4 Disparity Map Completion

We investigate the way of calculating a dense disparity map, from the disparity values of all pixels.

4.1 Dense map Completion

The method of completion is to use the disparity map with pixel precision (Image 7) after the left-right validation as initial disparity. First, we filter out isolated valid disparity values(more than four non valid disparity values in 8-connexity neighbor pixels). Then we take into account the fact that disparity is continue between two contours, and we filter out disparity values that do not conform to the gaussian probability distribution, according to the rule:

$$Probability(\bar{d} - (3.09 \cdot \sigma_d) < Disparity_w < \bar{d} + (3.09 \cdot \sigma_d)) = 0.998 \qquad (17)$$

where $\bar{d}$ is the mean and σ_d^2 the variance of disparity values in the 3x3 window centered on the disparity value to validate (the disparity value to validate is not used for the mean and variance computation). Next we by-pass totally isolated disparity value

(eight non valid disparity value), all this eliminates isolated bad values but not structured ones.
Now like previously, we fill up missing disparity values, by non-isotropic estimation from four connexity values. This is done for a maximal propagation distance. For example for a maximal distance of two pixels, we propagate a valid disparity estimation on the next two pixels in the four directions (up, down, left, right).
Let us follow the right propagation case:

- ☛ if the right neighbour pixel as a valid disparity his value is not modified and the new propagation value is its own disparity value corrected by the value of the disparity slope (estimated from previous values), propagated for two pixels more.
- ☛ If the right neighbour pixel has not a valid disparity, it receives the propagated value and so on, until next right neighbour pixel has a valid value or distance equal two.
- ☛ if the right neighbour pixel is a contour, propagation is stopped.

The same is done for the three other directions.
So, a pixel with non valid disparity value receives at most four propagated values (4-connexity), if all neighbours have a valid disparity. Finally it takes the mean value of all propagated values.This is done on left and right disparity maps. Then a new left-right validation is made to validate the new disparity values obtained from completion.
We stop the process when the maximum iteration is reached or until no more values from completion are validated (Image 9).

5 Kanade correction

At this point, we have a true localization of the disparity discontinuities on the dense initial map with pixel precision $D(P)$ and we may apply Kanade correction $\hat{\Delta}d$ on it with non constant window size [10][11] and [12], using:

Disparity variation factor α_d

$$\alpha_d = \frac{1}{N}\sum_{i=0}^{N-1}\frac{(D(x_i,y_i)-D(X,Y))^2}{dist((x_i,y_i)(X,Y))} \tag{18}$$

and Texturation factor α_f

$$\alpha_f = \frac{1}{N}\sum_{i=0}^{N-1}\frac{d}{dx}I_R(x_i+D(X,Y),y_i)^2 \tag{19}$$

in the expression of Incertitude on the Kanade correction $\sigma^2_{\hat{\Delta}d}$

$$\sigma^2_{\hat{\Delta}d} = \frac{1}{\sum_{i=0}^{N-1} \frac{\left(\frac{d}{dx} I_R(x_i + D(X,Y), y_i)\right)^2}{2\sigma_N^2 + dist((x_i, y_i)(X,Y))\alpha_d\alpha_f}} \tag{20}$$

This gives for each disparity value $D(P)$ Kanade correction $\hat{\Delta}d$ at each iteration until convergence, with:

$$Alphas(i) = \alpha_d\alpha_f \times dist((x_i, y_i)(X,Y)) \tag{21}$$

$$Intensity(i) = I_L(x_i, y_i) - I_R((x_i + D(X,Y)), y_i) \tag{22}$$

$$Derive(i) = \frac{d}{dx} I_R((x_i + D(X,Y)), y_i) \tag{23}$$

$$\hat{\Delta}d = \left(\sum_{i=0}^{Nbp_w - 1} \frac{Intensity(i) \times Derive(i)}{2\sigma_N^2 + Alphas(i)} \right) \times \sigma^2_{\hat{\Delta}d} \tag{24}$$

were Nbp_w is number of pixel in Kanade adaptive window.

Here we obtain a final dense disparity map in subpixel precision with good discontinuity location.

6 Experimental Results

The algorithm corresponding to the idea described in the previous section has been implemented and tested on aerial images 400x400 (Grand-Palais) with natural and artificial objects.

The most interesting characteristics of this image are that we find: Continuity in trees area. A lot of small dicontinuities like cars, isolated trees. Some occlusions due to car and people motions. Large occlusions and High discontinuities due to the building, and the fact that we are not in a polyhedric world(dome,...).

The classical disparity map by correlation with fixed window size 7x7 (Image 8) is compared to a map obtained by «limits of disparity»(Image 9), with adaptive window

limited by contours. All the isolated white and black spots in (Image 9) represent occulted or non matched pixels.

☛ For example on the floor: shadow from bushes in the garden or from the trees, car moving on the road, people in the garden, road lines occluded.

We have also tried the algorithm on 256x256 image of the Death Valley area (Image 12), 400x400 SHARMAH area (Image 10), 400x400 Ville-Franche town area (Image 13)(south of France), 512x512 Pentagon building (Image 15) and 600x600 picture of Paris center (Image 14).

We saw that σ_N may be found by computing standard deviation on the window from noise estimation using median filter [13] for each pixel. The introduction of this in our program give best matching if we use Lambertien model, but in most real images we find a lot of reflections, giving difference between left-right images greater than noise estimation. So to be less disturbed by reflection we use global estimation $\sigma_N \approx 10$.

Conclusion

In this paper, we show the effect of the contours constraint windows on correlation computation and the use of disparity limits as initial map of Kanade correction to have sub-pixel precision. We have tried many different way of window-size computation variation. Several experiments on «limits of disparity» with different edgels extractions remain to be done. The results already obtained are interesting (Image 11), and confirm that this technique of contour limitation is worth pursuing.

Acknowledgments

The authors would like to acknowledge Professor T.Kanade and M.Okutomi for helpful conversations, as Professor G.MEDIONI and the ISTAR Company for providing stereo pairs images.

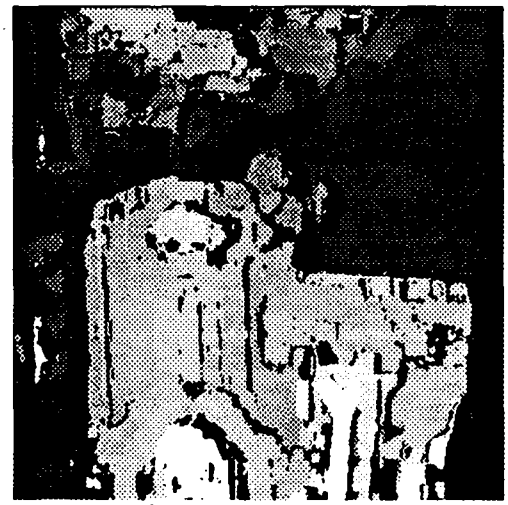

Image 8 Left Disparity map obtained by cross correlation with fixed window size 7x7.

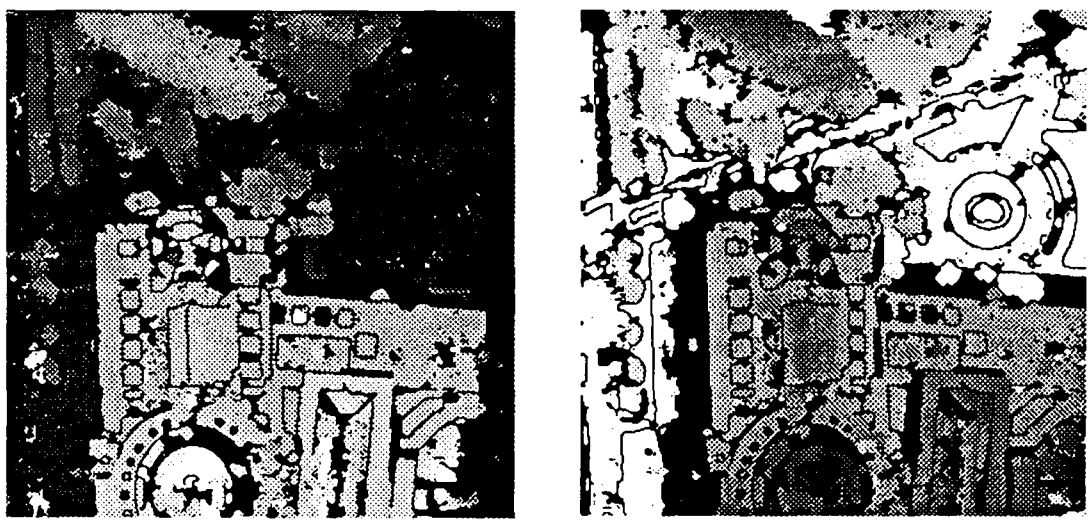

Image 9 Left and Right Disparity Limits with completion map.

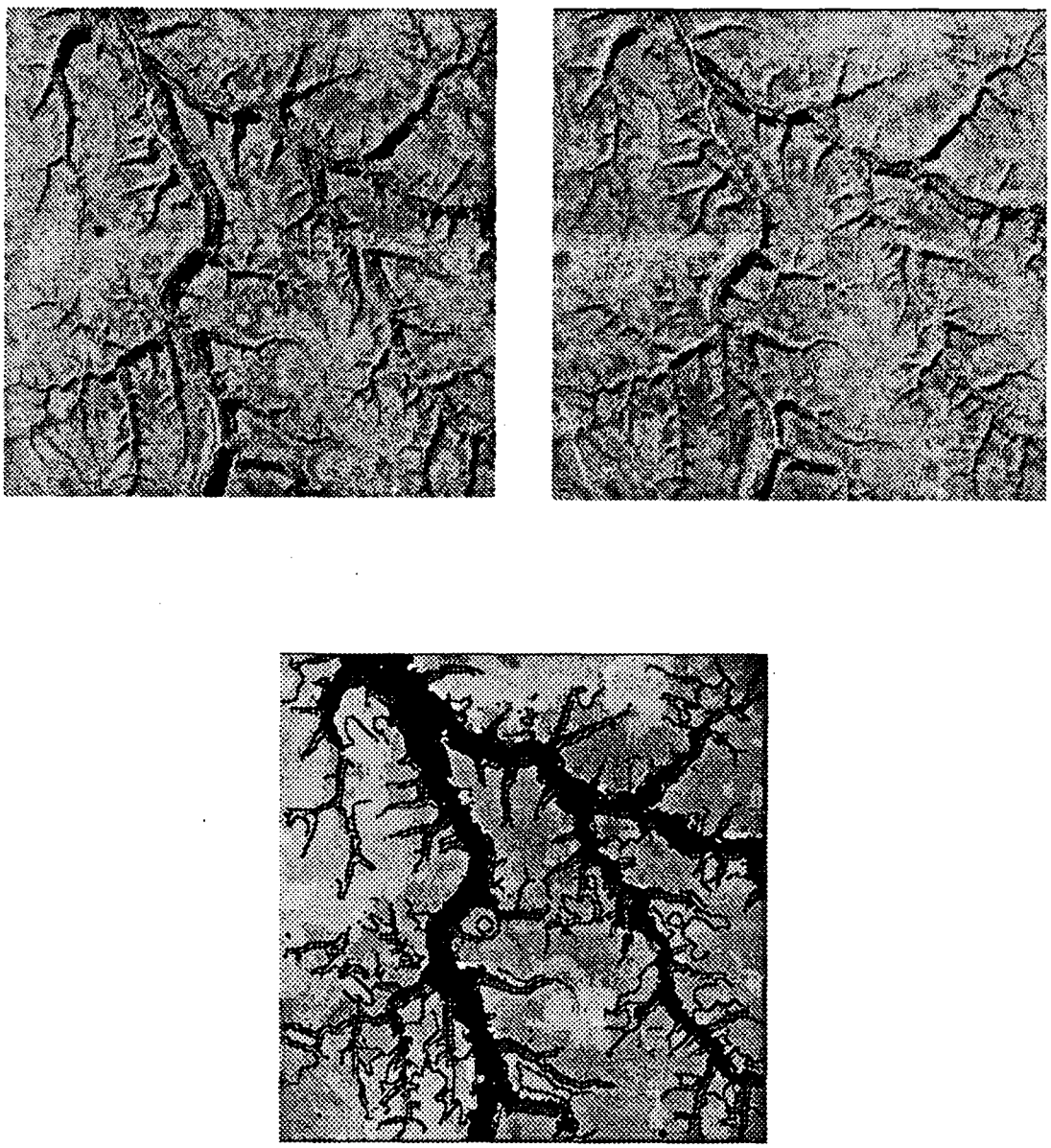

Image 10 400x400 image of Sharmah area, thresholding:
Noise=4, Texture=0.1, Correlation=0.7, d=[-10,5].

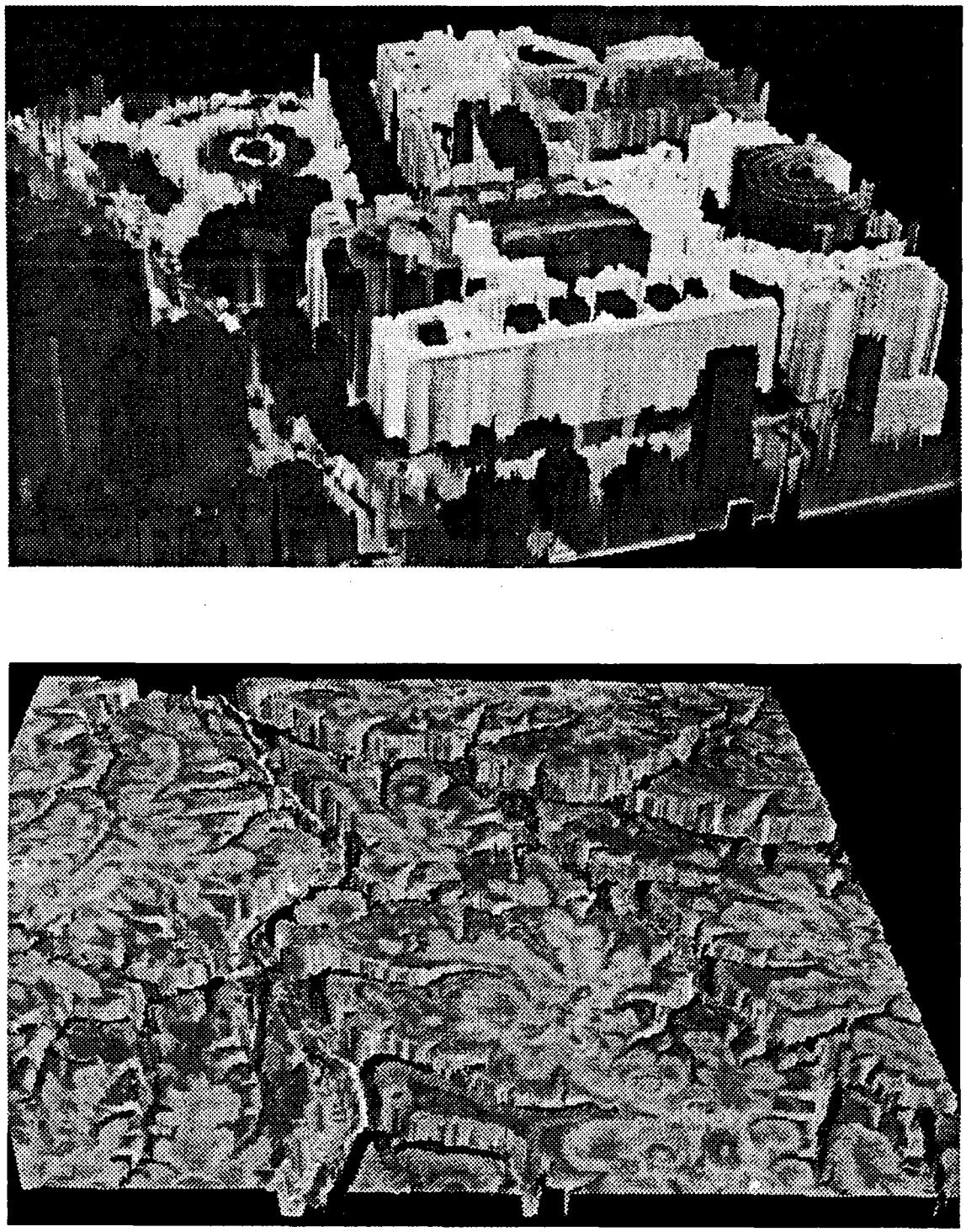

Image 11 Disparity Limits correlation map after completion, 3D representation.

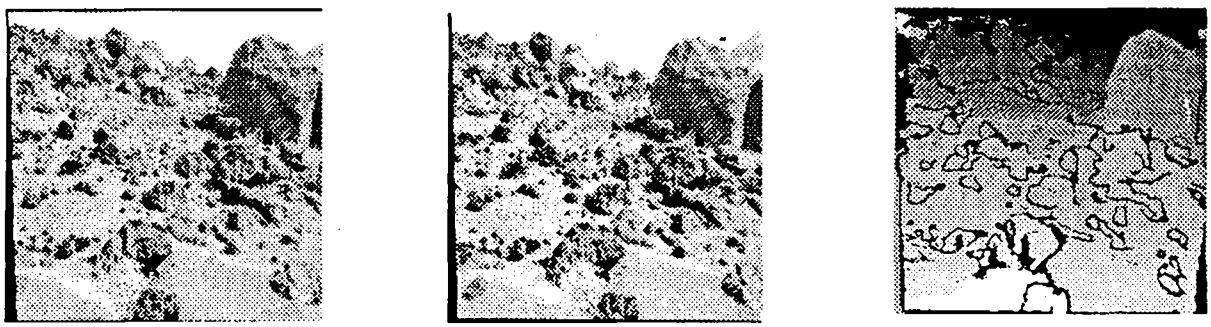

Image 12 256x256 image of Death Valley area, thresholding:
Noise=7, Texture=0.1, Correlation=0.7, d=[-17,16].

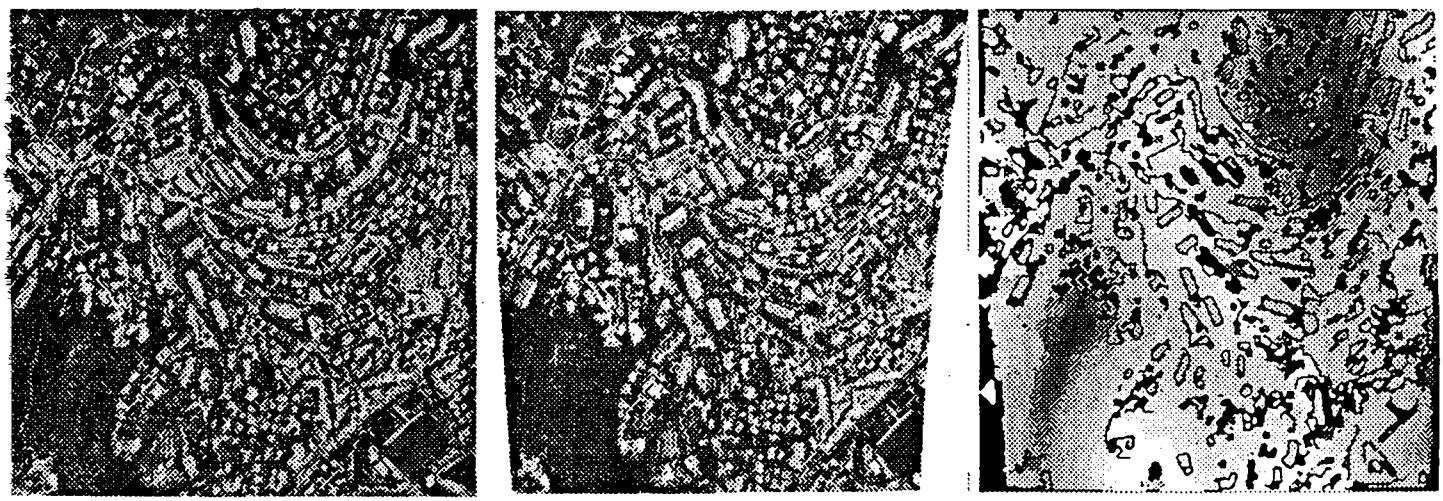

Image 13 400x400 image of Ville-franche area, thresholding:
Noise=7, d=[-10,10], Texture and Correlation non.

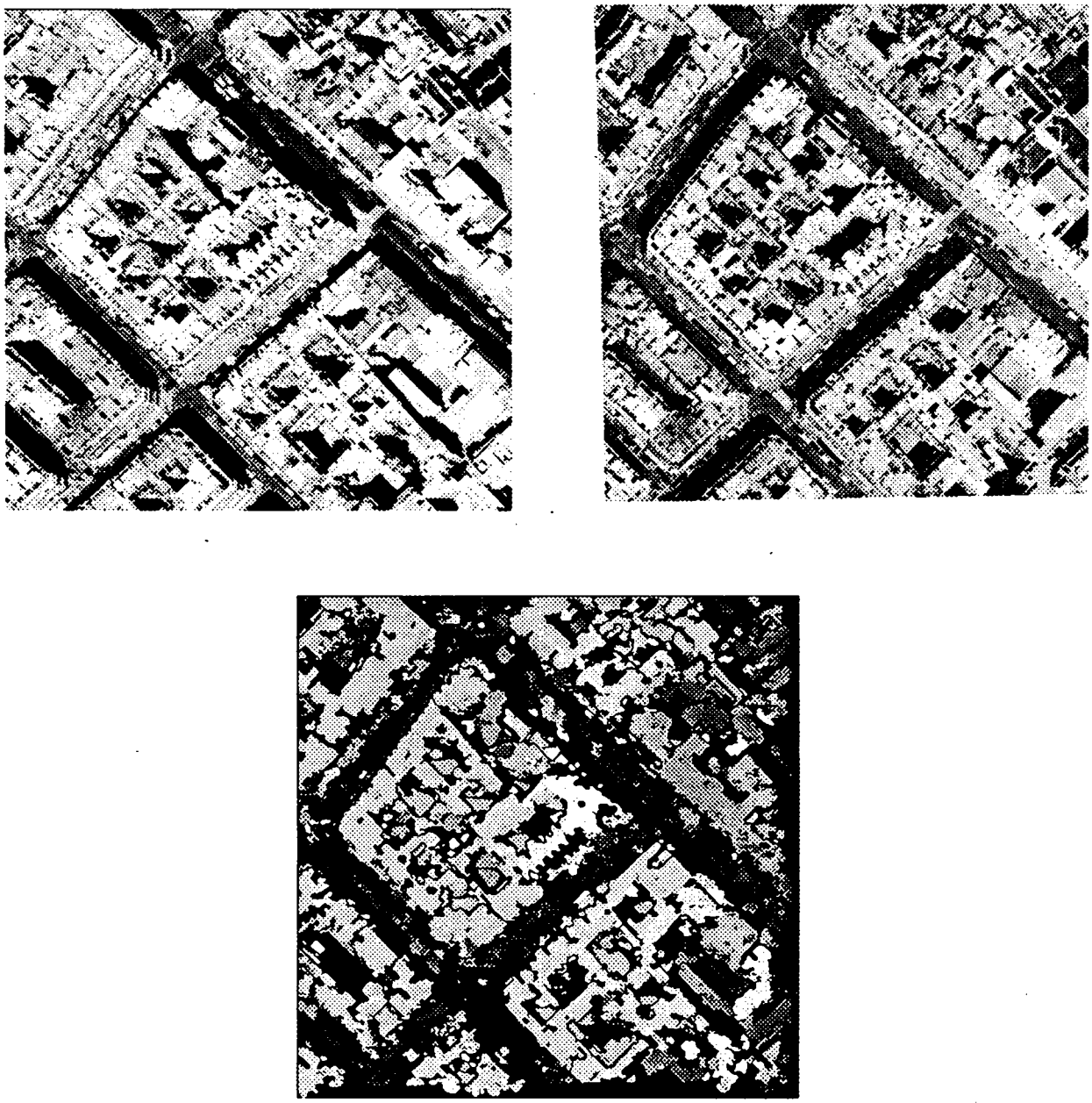

Image 14 600x600 image of Paris center, thresholding:
Noise=10, Texture=1.0, Correlation=0.7, d=[-1,40].

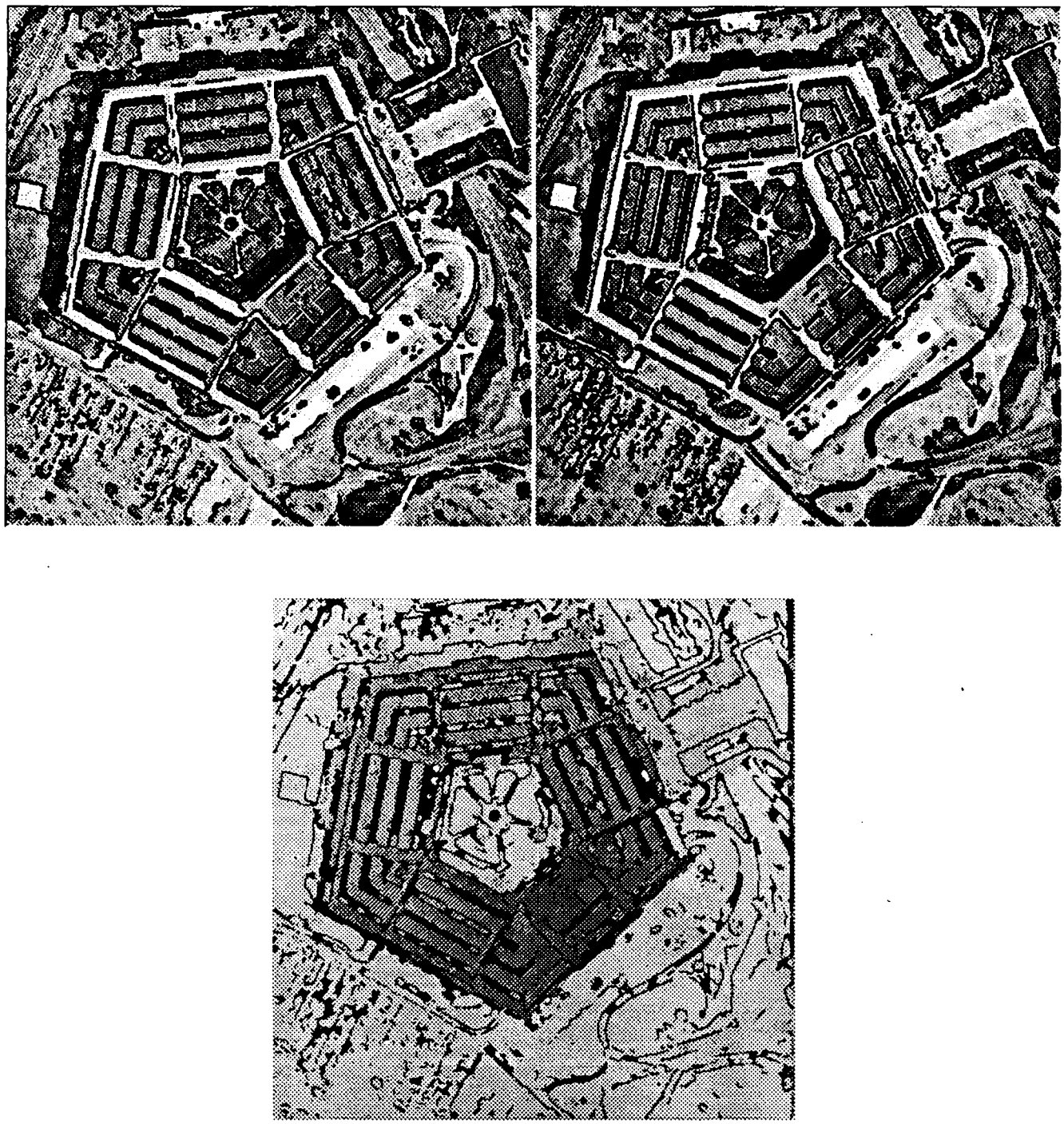

Image 15 512x512 image of Pentagon building, thresholding: Noise=10, Texture=0.5, Correlation=0.5, d=[-10,10].

References bibliographie

[1] N. Ayache, " Stereovision and sensor fusion ", M.I.T. Press, 1990.

[2] S. D. Cochran & G. Medioni, " 3-D Surface Description from Binocular Stereo ", IEEE PAMI Vol.14, No.10, 981-994, October 1992.

[3] R. C.-K. Chung & R. " Nevatia, Recovering Building Structures from Stereo ", IEEE CVPR 0-8186-2840-5/92 64-73, 1992.

[4] P.Fua, " A parallel stereo algorithm that produce dense depth maps and preserves images features ", INRIA Research Report No.1621, 1992.

[5] G.Giraudon, " The Local Extrema of Second Derivative as Stereo Feature ", CESTA, April 1986.

[6] D.Geiger, H.Bulthoff & A.L.Yuille, " Stereo Integration, Mean Field Theory and Psychophysics ", DARPA 73-82, 1992.

[7] B. Hotz, " Etude de Techniques de Stereovision par Correlation ", INRIA Research Report DEA, September 1991.

[8] W. Luo & H. Maître, " Using surface model to correct and fit disparity data in stereo vision ", IEEE ICPR Atlantic City, Vol.1, 60-64, June 1990.

[9] D.M. McKeown & Y.C. Hsieh, " Hierarchical Waveform Matching: A New Feature-Based Stereo Technique ", IEEE CVPR pages 513-519, 1992.

[10] M. Okutomi & T. Kanade, " A locally Adaptive Window for Signal Matching ", International Journal of Computer Vision 7:2, 143-162, 1992.

[11] M. Okutomi & T. Kanade, " A Stereo Matching Algorithm with an Adaptive Window Theory and Experiment ", Proc. Intern. Conf. Robot. Autom., 1088-1095, April 1991.

[12] M. Okutomi & T. Kanade, " CMU Technical Report ", CMU-CS-90-120, 1990.

[13] S.I. Olsen, " Estimation of Noise in Images: An Evaluation ", CVGIP Graphical Models and Image Processing Vol.55, No.4, 319-323, July 1993.

[14] L. Renouard, " Restitution automatique du relief à partir de couples stéréoscopiques d'images du satellite SPOT", PhD thesis, Ecole Polytechnique, France, July 1991.

[15] H.Voorhees & T.Poggio, " Detecting Textons and Texture Boundaries in Natural Images" , IEEE ICCV London, June 1987.

Unité de Recherche INRIA Sophia Antipolis
2004, route des Lucioles - B.P. 93 - 06902 SOPHIA ANTIPOLIS Cedex (France)

Unité de Recherche INRIA Lorraine Technopôle de Nancy-Brabois - Campus Scientifique
615, rue du Jardin Botanique - B.P. 101 - 54602 VILLERS LES NANCY Cedex (France)
Unité de Recherche INRIA Rennes IRISA, Campus Universitaire de Beaulieu 35042 RENNES Cedex (France)
Unité de Recherche INRIA Rhône-Alpes 46, avenue Félix Viallet - 38031 GRENOBLE Cedex (France)
Unité de Recherche INRIA Rocquencourt Domaine de Voluceau - Rocquencourt - B.P. 105 - 78153 LE CHESNAY Cedex (France)

EDITEUR
INRIA - Domaine de Voluceau - Rocquencourt - B.P. 105 - 78153 LE CHESNAY Cedex (France)

ISSN 0249 - 6399